Digital integral cloaking

Joseph S. Choi[1*] and John C. Howell[1,2,3,4]

[1]*The Institute of Optics, University of Rochester, Rochester, New York 14627, USA*

[2]*Department of Physics and Astronomy,*

University of Rochester, Rochester, New York 14627, USA

[3]*Center for Coherence and Quantum Optics,*

University of Rochester, Rochester, New York 14627, USA and

[4]*Institute for Quantum Studies, Chapman University, Orange, California 92866, USA*

Abstract

We propose 'digital cloaking' as a method for practical cloaking, where space, angle, spectrum, and phase are discretized. At the sacrifice of spatial resolution, a good approximation to an 'ideal' cloak can be achieved- a cloak that is omnidirectional, broadband, operational for the visible spectrum, three-dimensional (3D), and phase-matching for the light field, among other attributes. Experimentally, we demonstrate a two-dimensional (2D), planar, ray optics version of our proposed digital cloak by using lenticular lenses, similar to 'integral imaging' for 3D displays. With the continuing improvement in commercial digital technology, the resolution limitations of a digital cloak will be minimized, and a wearable cloak can be developed in the future.

INTRODUCTION

An 'ideal' invisibility cloak can be considered to be broadband, omnidirectional, 3D, macroscopic, operational in the visible spectrum, and with matching of phase for the full-field of light [1]. Scientific research into invisibility cloaking gained momentum with the initial omnidirectional cloaking designs that used artificial materials ('metamaterials') [2, 3]. These guide electromagnetic waves around a hidden object, using metamaterials that are specifically engineered with coordinate transformations, so they are called 'transformation optics' cloaks. Many interesting designs have resulted from transformation optics, but due to their narrow bandwidth, anisotropy, and manufacturing difficulties, practical cloaks have been challenging to build [4].

Broad bandwidth and omnidirectionality appear to be the main competing elements for ideal invisibility cloaking, as both seem unachievable simultaneously [5, 6]. Thus, to demonstrate cloaking, researchers have relaxed these or other ideal characteristics. Some of these efforts include broadband 'carpet cloaks' for visible light on reflective surfaces [7], unidirectional phase-matching cloaks [8], macroscopic ray optics cloaking [9, 10], a cylindrical cloak for light through a diffusive medium [11], or a cloak that achieves all in the small-angle regime [6].

In this work we propose 'digital cloaking' that is practical to build, and which utilizes commercially available technologies that are improving independently of any cloaking efforts. This is done by discretizing space, angle, spectrum, and phase, as an approximation to ideal cloaking. Since detectors, including imaging systems such as our eyes, are limited in resolution (spatially and temporally), digital cloaking can appear to be omnidirectional for a broad spectrum when observed. In fact, discretization of space is inherent in nature with atoms and molecules making up matter. Even metamaterial cloaking relies on discrete structures that are sub-wavelength in scale, to generate an averaging effect for the operational wavelength(s) [1]. For our digital cloak, we simply propose the discretization to be larger than atomic or wavelength scales, on the order of resolution limits of the observer, be it biological or a machine/device. For human visual acuity, resolution finer than about 30 arcseconds is sufficient [12].

The digital cloak we demonstrate is an 'active' device that requires external power input. However, passive discretized cloaking is also possible. Active cloaks have been proposed before, where the incoming signals are known a priori, or detected quickly, so that outgoing signals from antennas cancel the incoming wave(s) [13]. Other active cloaks, which compensate for

absorption and increase bandwidth, include using active metamaterial surfaces for dominant scattering cancellation, or using electronic circuits for acoustic cloaks [5]. These rely on custom-engineered material, whereas our digital cloaks can use commercially available technology. We believe this will be an advantage for scaling and implementation.

DISCRETIZED / DIGITAL CLOAKING

Invisibility cloaking makes the cloaked object appear transparent, as if the light fields exited the cloaked space *without* anything in it. It is a form of illusion, where light bends around the cloaked space, but re-forms afterwards to appear as if it had never bent. This allows both the cloaked object and the cloaking device to not only be hidden, but appear transparent [3, 10].

Let's begin with an ideal cloak (broadband, omnidirectional, 3D, phase-matching, etc.). We first make a 'ray optics' approximation, where the full phase of the electromagnetic field of light is not necessarily matched (We later show how to remove this approximation). For imaging, whether by camera or by the human eye, the phase is typically not detectable, which is why ray tracing is usually sufficient for designing imaging devices. Ray optics cloaking can be considered a discretization of spectrum and phase for a given ray, since its phase (modulo 2π) will match for one or more discrete frequencies, or discrete phase values can be matched for a given frequency. Ray optics alone significantly reduces the complexities of cloaking such that isotropic, off-the-shelf materials can be used to build macroscopic cloaks [10].

Figure 1(a) shows some rays that enter and exit an ideal, spherically symmetric cloak. We assume rotational symmetry (about $\mathbf{z}$), so only the cross-section of the spherical cloak is shown. For simplicity, only rays with one angle are shown, but due to spherical symmetry this implies that the cloak will work for all angles (omnidirectional). The dashed arrows show how the rays should *appear* to have traveled inside the cloak, which is to exit as if each ray propagated through the cloak in a straight line. In reality, the rays within the cloak should curve *around* an object or space that is intended to be invisible.

Building an omnidirectional cloak has been elusive to demonstrate, even for ray optics. For practical usage, since detectors including the human eye have finite resolution, the appearance for omnidirectionality can be achieved by discretizing space and momentum (or angle). We call this method of cloaking, '*discretized cloaking*.' A rotationally symmetric example is shown in
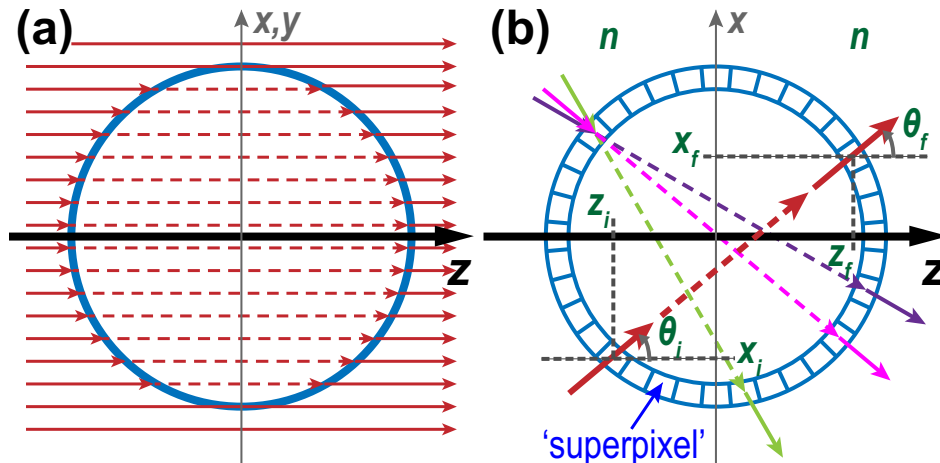
FIG. 1. **(a) Ideal, spherically symmetric cloak.** Example rays (solid arrows) that enter and exit the cloak (circle in 2D, sphere in 3D). Dashed arrows show how the rays *appear* to have traveled inside the cloak (where objects are invisible). Cloak is spherically symmetric, so it works for all ray angles (omnidirectional). **(b) Discretized, symmetric cloak.** Solid arrows depict a few sample rays of light entering and exiting. The surface of the cloak is discretized, so that each 'superpixel' in space can both detect and emit multiple, discrete ray positions and angles. A 'digital cloak' uses digital detection and display technologies for these discrete superpixels.

Figure 1(b), where each discretization in space is called a 'superpixel.' Each spatial 'superpixel' can contain separate 'pixels' that detect and/or display discrete ray angles. Additional 'pixels' may also be necessary for other ray characteristics. Discretized cloaking allows digital imaging and display technologies to be placed on the surface of the cloak. Utilizing such digital technology for cloaking is what we call '*digital cloaking.*' Strictly speaking, digital cloaking may discretize the spectrum of frequencies further than just the ray optics approximation. For example, some digital displays might only show red, green, and blue (RGB), so additional pixels/subpixels for discrete color may be required.

Implementing a discretized cloak or a digital cloak requires propagating the rays from input to output correctly. This can be done using the 'paraxial cloaking' matrix (Equation (1) of Ref. [10]), since the final ABCD matrix is still valid outside of the 'paraxial' (small-angle) regime. This is also shown in Figure 1(b), where given a transverse position y_i, angle θ_i, and longitudinal position z_i of the input ray, the output ray is given by (with same variable names

but with subfix '$_f$'):

$$\begin{bmatrix} y_f \\ n\tan\theta_f \end{bmatrix}_{z=z_f} = \begin{bmatrix} 1 & (z_f - z_i)/n \\ 0 & 1 \end{bmatrix} \begin{bmatrix} y_i \\ n\tan\theta_i \end{bmatrix}_{z=z_i}. \tag{1}$$

We have assumed rotational symmetry about the center axis ($\mathbf{z}$) and that the ambient medium has refractive index n. Note that each ray has its own longitudinal distance $L = (z_f - z_i)$ that is dependent on its input and output planes for the cloak. To be direct, we have used the 'real' angle θ instead of the 'paraxial angle' $u(= \tan\theta)$. Although Figure 1(b) shows a cloak that is circular in 2D, or spherical in 3D, arbitrarily shaped discretized cloaks are possible. For cloaks with general shapes, Equation (1) can be applied for each 2D plane containing the $\mathbf{z}$-axis.

DEMONSTRATION OF AN 'INTEGRAL CLOAK'

We now present and demonstrate a method for digital cloaking. As described previously, the key to digital cloaking and discretized cloaking is to detect and reproduce proper ray positions and angles. One way to achieve this is to utilize 'Shack-Hartmann' wavefront sensors, or 'fly's eye' lens arrays. These allow the position and momentum of rays to be captured by using arrays of small lenses, which can spatially separate rays of different angles (See Figure 2(a)). Remarkably, Lippmann had proposed photography using this concept in 1908, and attempted to demonstrate this 'integral photography' with limited technology [14]. Resolution, depth of field, and limited viewing angles are typically drawbacks for 'integral' 3D displays, but improvements are being made [15]. In particular, with current commercial efforts to increase the pixel density of displays, we anticipate resolution to improve continually. For cloaking, we can use lens arrays on a display panel to generate the desired ray output pattern according to Equation (1).

Micro-lenslet arrays have been suggested previously for transformation optics by the Courtial group [16]. They use two pairs of lenslet arrays in a confocal setting (both focal planes overlapping), as a 'window' that can refract light passing through. They have suggested using these pairs of arrays as the building blocks for a passive cloaking device, where the object inside appears shrunk. So far, they have simulated such effects only [17].

We term '*integral cloaking*' to be cloaking that uses integral imaging techniques. An example implementation is shown in Figure 2(b). For purposes of demonstration, we simplified with two
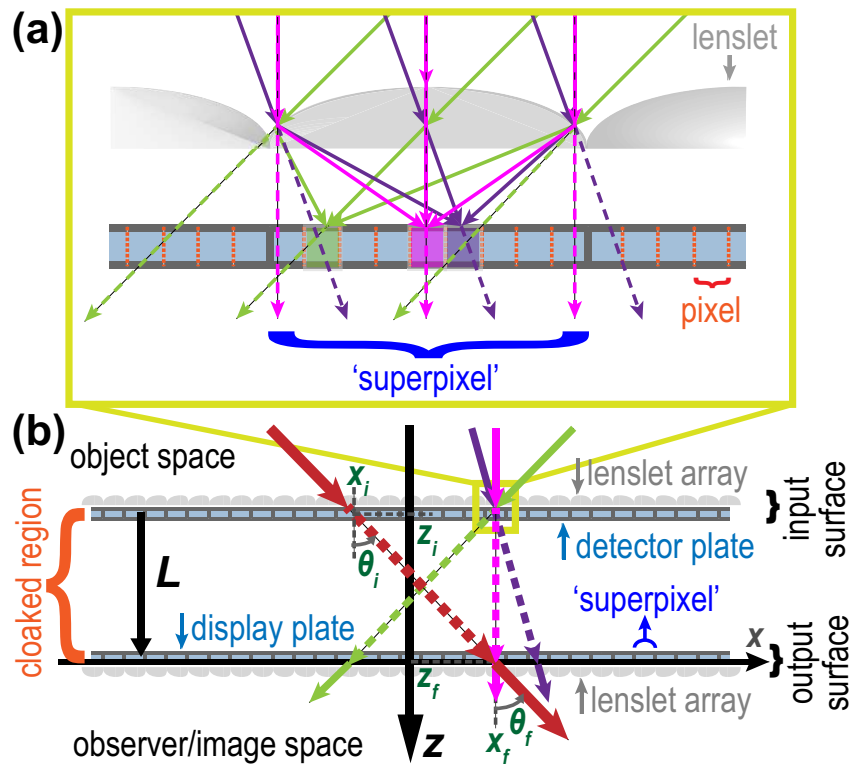
FIG. 2. **(a) Integral imaging detection.** (Zoomed out portion of **(b)**). Each 'pixel' detects one unique ray position and angle. A 'superpixel,' placed at the focusing plane of a lenslet, collects rays with the same position as the lens. These rays are then spatially separated into 'pixels,' such that one ray angle (or 'view') maps to one pixel. Display (output) is the reverse of detection scheme shown here. **(b) An 'integral cloak.'** Cross-section of two parallel, 2D surfaces, with a few sample rays. The input 'surface' (lens array + plate) captures input light rays. Output surface displays rays as if they passed through ambient space only (dashed lines).

parallel plates and two lenslet arrays, where we captured rays with one plate and displayed rays with the other, only. With parallel plates, $L = (z_f - z_i)$ is constant in Equation (1) for all rays. To simplify the required equipment, we also limited our cloak to 2D, where observers are at a fixed height, and move only in the plane horizontal to the floor (**x-z** plane in Figure 2(b)). Since both eyes of an observer typically lie on the same horizontal plane, stereoscopic depth

can still be perceived with the 2D version. Integral cloaking in the vertical plane follows the same principles, just rotated, so that in algorithm and in theory, 2D cloaking extends to 3D in a relatively straightforward manner.

Figures 3(a) and 3(b) show the setup for our 2D integral cloak. The input plane (input camera sensor on slider) and display screen were separated by $L = 13$ cm. The cloakable volume behind the active display screen was then ~ 2500 cm^3. The background objects consisted of four sets of colored blocks, the total depth of the object space (from the input plane) being 90 cm. Rays from the input camera are 'propagated' by a computer to the output.

For the image capture (input) plane, we used a digital camera (Sony DSC-RX10), mounted on a mechanical slider that scans horizontally at a fixed speed Each camera frame represented a single lenslet and 'superpixel' (of the input surface in Figure 2(b)) located at the instantaneous camera position (x_i, y_i). The camera image pixels then corresponded to the detector 'pixels,' shown in Figure 2(a). From the camera field-of-view, we could then calculate the input ray angles (θ_i) for these pixels. Knowing the input ray position and angle, a computer then propagated the ray to the correct output pixel using Equation (1).

For 2D, a scanning camera was not only easier to obtain than a combination of lenslet and detector arrays (input surface of Figure 2(b)), but it had improved performance. This is because a continuous scan gave a horizontal spatial resolution of 0.106 mm in camera positions. This was about 10 times better than the horizontal spatial resolution of our final system (1.34 mm), which was set by the output lenslet array. In addition, commercial cameras are highly aberration-corrected, whereas lenslet arrays usually have little, if any, corrections; this causes the former to have sharp images, both for input and output.

The benefits of our horizontal scanning method come at the cost of a delay in time. For our setup (Figure 3), the input scan required 29 seconds, and the computational processing required 22 seconds on the laptop that ran our code. We required additional time to test and transfer data, but with proper hardware interfacing, this can be automated with little delay. Both scan and processing times increase with the dimensions of the cloakable volume. For example, the horizontal scan distance required is $(Ws + 2L \tan(FOV_l/2))$. Here, W_s is the active screen width of the output display, and FOV_l is the field-of-view (FOV) of the output lenslet array. Subjective quality requirements of the cloak can dictate the speed as well. A 3D version would

require raster scanning over a 2D (**x-y**) plane, which can be difficult and time-consuming, if using a single camera. Thus, for real-time or 3D digital cloaking, using a 2D array of detectors combined with a fly's eye lenslet array (Figure 2(b)) for the input surface would be the practical, though likely costly, approach.

We now describe the display (output) plane of our cloak. For the output display, we used a 20 cm (diagonal) LCD monitor (Apple iPad mini 4). Our output lenslet array was a 2D cylindrical lenslet array (20 lens-per-inch array from Micro Lens Technology). Both display monitor and lenslet array were commercially available. For a 3D integral cloak, a fly's eye lens array should replace the cylindrical lenslet array. By slanting the cylindrical lenses, we utilized the 3 RGB subpixels to gain 3 times the horizontal angular resolution (in number of 'views'), at the sacrifice of vertical resolution [15]. Our output system generated 51.5 discrete 'views' over 29° of viewing angles (field-of-view), horizontally. This 29° was the field-of-view of the lenslet array (FOV_l), and limited the cone of angles for both the output and input of our cloaking system, since the input camera field-of-view was larger ($\sim$60°). Each 'view' corresponds to a discrete ray angle/momentum (one 'pixel' in Figure 2(a)) that is displayed for our system. This determined the output angular resolution of our cloaking system, giving 0.56° between neighboring views. Note that this output 'angular resolution' of the digital integral cloak is how much an observer must move to see a change in image (corresponding to the subsequent 'view'). So smaller angular resolution values provide more continuous viewing, and allow farther observation distances, than larger values.

Figures 3(c)-(f) show a horizontal (**x**) demonstration of this 2D integral cloak. An "observer" camera at a fixed height (y) near the center of the cloak, and fixed distance z from the cloak, was placed on a slider to scan horizontally (x). This camera was 260 cm from the display screen (cloak). Figures 3(c)-(f) show 10.8° viewing range. The objects behind the cloak match in horizontal alignment, size (magnification), and parallax motion for varying object depths (from the cloak). As expected for real 3D scenery, the objects that are farther from the screen move across the cloaking screen quicker than those closer to the screen.

The vertical magnification was matched for a particular observer distance and object depth combination, since this was a 2D cloak that used cylindrical lenses. In our case, from the observation distances we used, as in Figures 3(c)-(f), the vertical sizes of objects near the
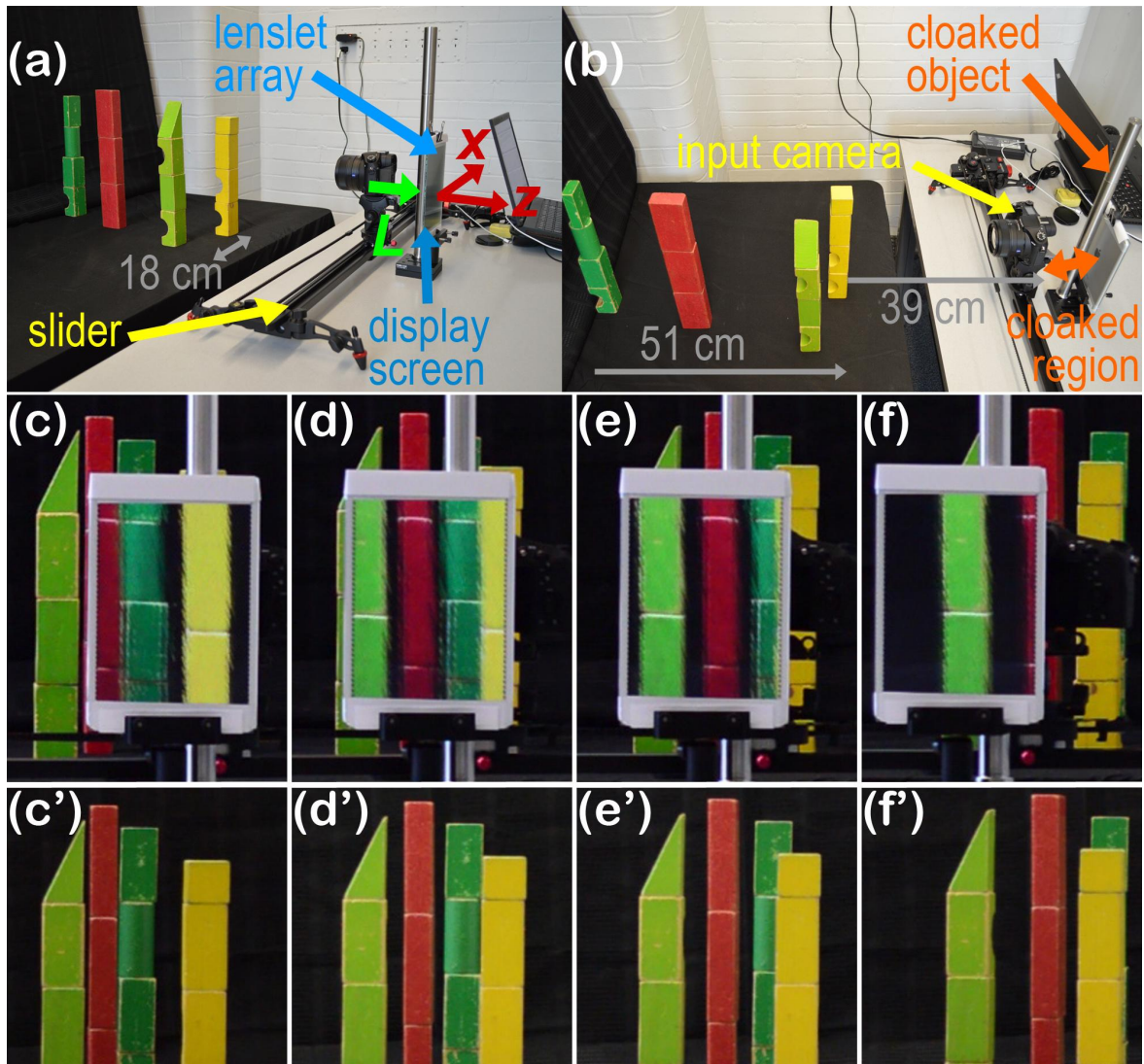
FIG. 3. **(a)-(b) 2D integral cloak setup.** The input camera on a slider (input plane) scans horizontally to gather input rays. The lenslet array on the display screen (output plane) together emit rays according to Equation (1). The space between the input and output planes (separated by L) is the cloaked region. **(c)-(f)** *With* **the integral cloak.** Screen shots by an "observer" camera that moved horizontally. Viewing angles from screen center to observer camera: **(c)** $-4.1°$, **(d)** $0.0°$, **(e)** $2.0°$, **(f)** $6.7°$. **(c')-(f')** *Without* **the integral cloak.** The cloaking screen, in **(c)-(f)**, horizontally matches **(c')-(f')** respectively, in size, alignment, and parallax motion.
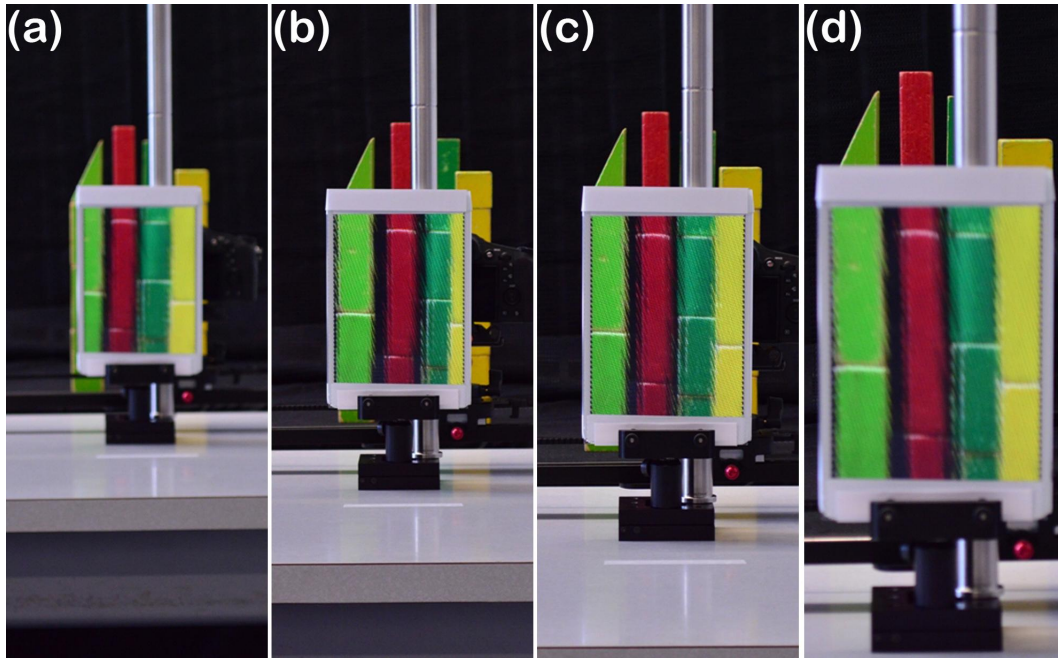
FIG. 4. **(a)-(d) Integral cloak longitudinal (z) demonstration.** Observer (camera) at different distances in front of the display screen of the cloak: 272 cm, 235 cm, 203 cm, and 150 cm, for (a)-(d), respectively. As expected, the cloak displays more of the background objects, spatially, for closer observation.

farthest blocks (dark green) and red blocks were roughly matched. However, if spherical fly's eye lenslet arrays are used for a full 3D integral cloak, the vertical alignment and magnification will match for all object and observer distances, in theory.

Figures 4(a)-(d) show a longitudinal ($\mathbf{z}$) demonstration of our integral cloak, by varying observation distances away from the cloaking screen. The horizontal field-of-view occupied by the cloaking screen, from the observer camera, were 2.53°, 2.93°, 3.38°, 4.59°, for Figures 4(a)-(d), respectively. This is the range of angles ('views') of the light rays that the observer camera captures. As an observer moves closer to the cloak (towards Figure 4(d) from Figure 4(a)), a larger range of angles is seen. This corresponds to a larger spatial amount of the background scene being shown by the cloak (horizontally). For a cloaking system, which should appear as if absent (transparent), this is as expected.

Finally, we characterize our digital integral cloak with additional quality metrics. Since ours was a 2D demonstration, we limited our analysis to the horizontal ($\mathbf{x}$) and longitudinal

(**z**) dimensions. The horizontal input angular resolution for our system was 0.031°, which corresponds to the uncertainty in the input ray angles. (Recall the output angular resolution was 0.56°.) To provide sufficient depth-of-field, we stopped-down our input camera to f-number = f/10. The resulting input aperture diameter was then 0.88 mm (effective lenslet diameter in Figure 2(a)). This corresponds to the range of transverse spatial positions, of the objects, that are captured for each detector pixel of the input camera. Comparatively, the output aperture was 1.34 mm.

Our demonstrated depth-of-field was over 60 cm, such that all the objects we demonstrated for the cloak (Figures 3 and 4) were at least in good focus when collected for input. The input camera was not the limiting factor here, as we could achieve several meters depth-of-field, but the display (output) surface limited the resolution to display object depths clearly. The spatial sensitivity of our slanted lenslet array to be misaligned on the display is such that a 0.026 mm change in position will shift the 'view' seen. The angular sensitivity of the lenslet array alignment with respect to the display screen pixels was $(8.8 \times 10^{-3})°$.

DISCUSSION

Our digital cloak demonstration was dynamic, so that a changing background could be displayed properly, after a finite lag time for scanning and processing. Work to make a real-time cloak is underway. Depending on the length scales for how the cloak is to be observed, the requirements for detection and output can change. For example, if the observer is far away from the cloak, then large screens with low resolution can be sufficient.

The phase of the light fields can be matched by including properly engineered materials for a fixed-shape cloak, or spatial light modulator arrays for a cloak with dynamic shapes. If we assume each pixel corresponds to a single ray position, angle, frequency, it is straightforward to trace an input pixel to its output pixel (Equation (1)). To good approximation, each pair is then a unidirectional propagation from input pixel to output pixel (dashed lines in Figure 2), with respect to a new **z**-axis. This allows the paraxial full-field cloaking theory to be used for each pixel pair, to calculate the phase and dispersion necessary for phase-matching of light fields [6]. These assumptions and approximations become increasingly accurate as the cloak pixel size decreases.
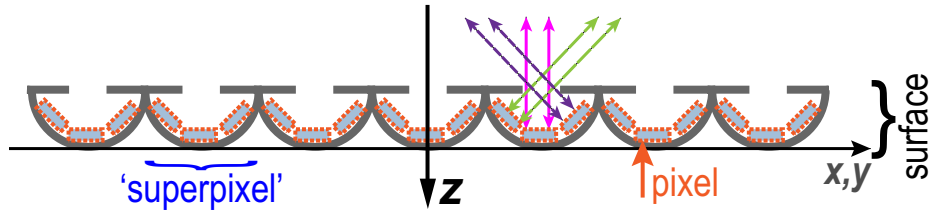
FIG. 5. **Lensless 'integral cloaking' surface.** Cross-section view shown. Detector and/or display pixels can be placed on curved 'superpixels.' The top layer, which has holes for rays to pass, can be made to absorb light, or also detect incident light to calculate and compensate for irradiance losses.

We suggest a few other methods for discretized cloaking. Optical fibers or other optics, with good anti-reflection coatings, can be used to collect and transmit analog measurement values. Some advantages of this include cloaking in a passive (rather than active) manner, and that its spectrum can be continuously broadband. Additionally, a discretized cloak without lenses is possible by using curved surfaces for detection and emission of rays. This is similar to one of the original methods proposed by Lippman for integral photography [18]. An example surface of such a cloak is shown in Figure 5. This method might be easier to mass-produce and align than integral cloaking with lenses, and its field-of-view will not be limited by lens curvatures (although limited in other ways).

Lastly, with increased computational power and refined resolution, digital cloaking can be adapted to be wearable. Sensors can be used to determine the position and orientation for each pixel, with a processor calculating the correct ray propagation (Equation (1)) and output pixel. This will allow for cloaks that are dynamic in shape.

In conclusion, to approximate an ideal cloak for practical observation, we have proposed discretized cloaking. In particular, we have demonstrated a 2D digital integral cloak, by using commercially available technologies- A camera to capture the input rays, and a monitor + cylindrical lenslet array for the output rays. Our demonstration had 0.56° angular resolution over 29° field-of-view, and spatial resolution of 1.34 mm, limited by the output system. The principles for generating a 3D integral cloak follow easily. Although our demonstration was for ray optics cloaking, we have suggested other designs, including methods to match the phase of the light fields. Digital cloaking has good potential for wide implementation as a wearable cloak, since the digital technology required continue to improve commercially.

---

* Corresponding author. joseph.choi@rochester.edu

[1] G. Gbur, Progress in Optics **58**, 65 (2013).

[2] J. B. Pendry, D. Schurig, and D. R. Smith, Science **312**, 1780 (2006).

[3] U. Leonhardt, Science **312**, 1777 (2006).

[4] M. McCall, Contemporary Physics **54**, 273 (2013).

[5] R. Fleury, F. Monticone, and A. Alu, Physical Review Applied **4**, 037001 (2015).

[6] J. S. Choi and J. C. Howell, Optics Express **23**, 15857 (2015).

[7] J. S. Li and J. B. Pendry, Physical Review Letters **101**, 203901 (2008).

[8] N. Landy and D. R. Smith, Nature Materials **12**, 25 (2013).

[9] J. C. Howell, J. B. Howell, and J. S. Choi, Applied Optics **53**, 1958 (2014).

[10] J. S. Choi and J. C. Howell, Optics Express **22**, 29465 (2014).

[11] R. Schittny, M. Kadic, T. Bueckmann, and M. Wegener, Science **345**, 427 (2014).

[12] M. Bass, J. M. Enoch, and V. Lakshminarayanan, *Vision and vision optics*, 3rd ed., Handbook of optics, Vol. 3 (McGraw-Hill, New York, 2010).

[13] F. G. Vasquez, G. W. Milton, and D. Onofrei, Physical Review Letters **103**, 073901 (2009).

[14] G. Lippmann, C. R. Acad. Sci. **146**, 446 (1908).

[15] J. Geng, Advances in Optics and Photonics **5**, 456 (2013).

[16] A. C. Hamilton and J. Courtial, Journal of Optics A: Pure and Applied Optics **11**, 065502 (2009).

[17] S. Oxburgh, C. D. White, G. Antoniou, E. Orife, and J. Courtial (Proc. of SPIE, 2014) p. 91931E.

[18] Scientific American **105**, 164 (1911).